

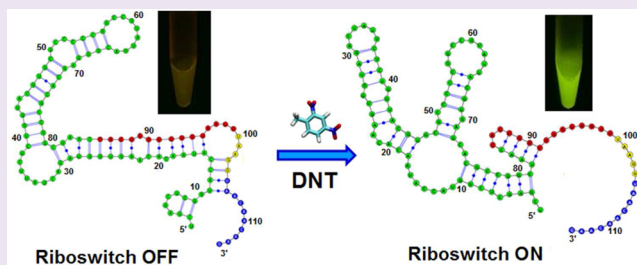
Development of a 2,4-Dinitrotoluene-Responsive Synthetic Riboswitch in *E. coli* Cells

Molly E. Davidson,[†] Svetlana V. Harbaugh,^{*,‡} Yaroslav G. Chushak,[‡] Morley O. Stone,
and Nancy Kelley-Loughnane^{*}

711th Human Performance Wing, Human Effectiveness Directorate, Air Force Research Laboratory, Wright-Patterson AFB, Ohio 45433, United States

S Supporting Information

ABSTRACT: Riboswitches are RNA sequences that regulate expression of associated downstream genes in response to the presence or absence of specific small molecules. A novel riboswitch that activates protein translation in *E. coli* cells in response to 2,4-dinitrotoluene (DNT) has been engineered. A plasmid library was constructed by incorporation of 30 degenerate bases between a previously described trinitrotoluene aptamer and the ribosome binding site. Screening was performed by placing the riboswitch library upstream of the Tobacco Etch Virus (TEV) protease coding sequence in one plasmid; a second plasmid encoded a FRET-based construct linked with a peptide containing the TEV protease cleavage site. Addition of DNT to bacterial culture activated the riboswitch, initiating translation of TEV protease. In turn, the protease cleaved the linker in the FRET-based fusion protein, causing a change in fluorescence. This new riboswitch exhibited a 10-fold increase in fluorescence in the presence of 0.5 mM DNT compared to the system without target.



Riboswitches are naturally occurring genetic regulatory elements found in the 5' untranslated region of some mRNA. They provide a method for cellular response to the presence or absence of metabolites by regulating the expression of downstream genes. Numerous examples of naturally occurring bacterial riboswitches have been discovered (reviewed in ref 1). The size and structure of metabolite targets vary significantly, an indication that riboswitches could be used to detect a wide range of targets.² This apparent versatility of riboswitches in nature is being exploited by researchers in order to develop synthetic riboswitches that regulate gene expression in response to desired target molecules. The advantage of such engineered riboswitches is that they offer a way to control gene expression *via* small molecules, *e.g.*, metabolites or drug compounds.

Riboswitch-containing cells are appealing as sensors because they are self-replicating and have the potential to sense a target for an extended period of time, over the life of the cell culture. In many instances, it may be easier to preserve bacterial cell function than to preserve antibody structure or enzymatic activity for sensing purposes. For example, antibodies are highly sensitive to pH, temperature changes, and variation in salt concentration. Bacteria, however, can function under a broader range of conditions and may be protected from environmental threats *via* hardening of the sensor system to increase operational lifetime, improve portability, and preserve function of cells.^{3–6} It should be noted that there are some conditions under which bacterial cell function is compromised, such as extreme temperature, pH, and/or salt concentration. On the

other hand, some riboswitches have been shown to act as thermosensors, responding specifically to temperature increases by becoming active and turning on transcription of specific genes that improve survival in high temperatures. One such riboswitch, responsible for regulating Mg²⁺ transport, was found in *Salmonella enterica*.⁷

Riboswitches are composed of two functional elements: a biological recognition element (aptamer) and an expression platform. The aptamer binds specifically to a small-molecule target, which induces a conformational change that leads to changes in gene expression. There are a number of mechanisms through which a riboswitch may produce changes in gene and protein expression, including regulation of transcription termination,⁸ translation initiation,⁹ or cleavage of mRNA¹⁰ (for review see refs 1 and 9). For sensing applications riboswitch activation should produce a positive signal when the aptamer binds the target. Ideally, the increase in signal intensity will be proportional to the amount of target detected by the system, as this provides a mechanism for quantification of the target.

Aptamers that recognize specific target molecules have been selected using techniques such as Systematic Evolution of Ligands by EXponential Enrichment (SELEX)¹¹ and allosteric selection.¹² Linking a specifically selected aptamer with an

Received: June 1, 2012

Accepted: October 23, 2012

Published: October 23, 2012

expression platform may yield a novel riboswitch that is active in cells and could be used to detect a molecule of interest.^{2,13,14}

Recently, Ehrentreich-Forster and colleagues selected and tested 2,4,6-trinitrotoluene (TNT)-specific aptamer for use in explosives sensing devices.¹⁵ They developed a method for detection of TNT utilizing a flow cell with immobilized TNT and fluorescently labeled aptamer that exhibited a decrease in fluorescent signal when TNT was present in the sample. We coupled this aptamer with a partially randomized expression platform to develop a riboswitch for the detection of a TNT structural analogue, 2,4-dinitrotoluene (DNT). DNT differs from TNT in that it lacks the presence of a third nitro group. We assumed that the lack of the third nitro group would not have a drastic affect on the binding ability of DNT to the aptamer. Further, since the riboswitch described in this work is based on the TNT aptamer, it should recognize TNT (as well as DNT, used herein as a surrogate).

2,4-Dinitrotoluene is an explosive chemical that is used in the production of the polyurethane foam for bedding and furniture industries and as a gelating agent in explosives, ammunition, and dyes.¹⁶ The detection of DNT is important for a few reasons. First, from a security perspective, DNT is an intermediate in the production of TNT, the most commonly used explosive in the world, and is released in the effluent following TNT manufacturing. The presence of DNT (concentration range of 0.04–48.6 mg/L) was detected with 100% rate of occurrence in wastewater samples ($n = 54$) collected from the effluent pipe of TNT production facility.¹⁷ Detection of DNT in a location could be an indicator of terrorist activity. Second, DNT from industrial waste can remain in soil and bodies of water for extended periods of time, posing a risk for humans and animals that are exposed. The toxic effects of DNT have been observed in bacteria, fish, reptiles, and other animals that act as indicators of toxicity in humans.^{16,18–21} Dangers associated with DNT exposure include immunosuppression, smooth muscle cell damage, and circulatory and cardiovascular problems.²²

This article describes the development of a synthetic riboswitch in *E. coli* cells that enables detection of DNT. An aptamer selected to bind TNT molecules¹⁵ was linked with a PCR-generated expression platform library placed upstream of the gene encoding Tobacco Etch Virus (TEV) protease. The riboswitch sensor output is based on the principle of Fluorescence Resonance Energy Transfer (FRET). Briefly, enhanced green fluorescent protein (eGFP) was linked to a non-fluorescent mutant yellow fluorescent protein called REACH (Resonance Energy Accepting Chromoprotein).²³ Use of this type of FRET pair eliminates acceptor fluorescence, and therefore little to no fluorescence is observed prior to cleavage.²⁴ The linker between these two proteins contains the TEV protease cleavage site. Upon activation of the riboswitch, TEV protease is translated and cleaves the FRET linker, allowing the detection of eGFP fluorescence. The selected riboswitch exhibited a 10-fold increase in fluorescence in the presence of 0.5 mM DNT compared to the system without target.

RESULTS AND DISCUSSION

We used a previously described TNT binding RNA¹⁵ ($K_d = 1 \times 10^{-8}$ M) as an aptamer domain to develop a synthetic riboswitch to detect the TNT structural analogue DNT. In order to determine the concentration of analyte suitable for riboswitch selection, and considering the high toxicity of 2,4-

dinitrotoluene to prokaryotic, plant, and mammalian cells,^{28,29} we tested the effect of different concentrations of DNT on the growth of *E. coli* cells. Concentrations of DNT higher than 1 mM were toxic for *E. coli* cells, resulting in complete suppression of cell growth (as shown in Supplementary Figure SI.1). DNT concentration of 0.5 mM slowed down the growth of cells but did not change the growth curve (compared to cells without DNT) and was chosen for riboswitch selection.

Construction of the Riboswitch Library. Using a polymerase chain reaction, we constructed a riboswitch library by incorporating up to 30 degenerate bases between the TNT aptamer and ribosome binding site (RBS) (Figure 1). The

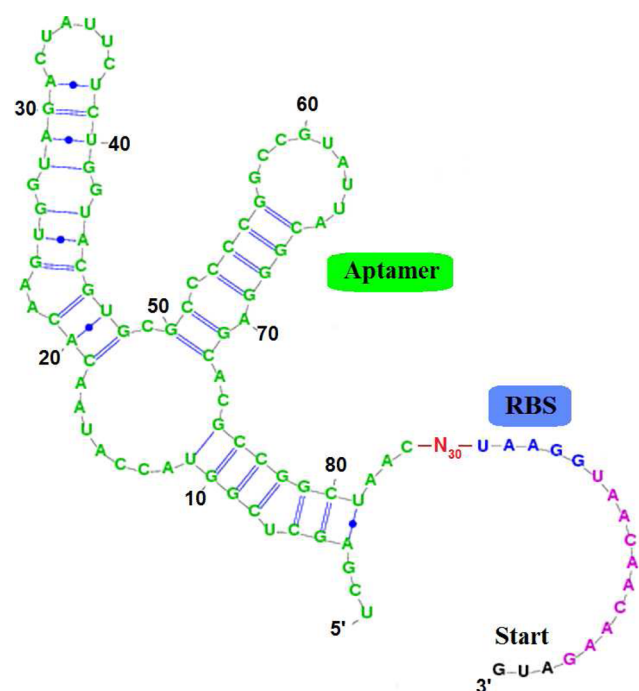


Figure 1. Construction of the riboswitch library. Thirty random bases (red) were inserted between the TNT specific aptamer (green) and ribosome binding site (RBS, blue) by PCR. The secondary structure of the TNT aptamer was predicted using Mfold software.

riboswitch library was placed upstream of TEV protease encoding sequence under control of the *tac* promoter and co-transformed (with a plasmid encoding FRET-based TEV protease substrate) into *E. coli* TOP10 cells, yielding approximately 1000 clones. It should be noted that transformation efficiency was modest due to usage of two plasmids and their large size (5,378 and 3,570 bp).³⁰ The largest colonies (627 were identified) that showed sufficient growth in the presence of analyte were used for screening. Our screening assay was based on a previously described system including TEV protease and FRET-based substrate production within the same cell.²⁴ In the absence of analyte, the translation of TEV protease is suppressed, the FRET-based protein substrate remains uncleaved, and cells do not show significant emission at 510 nm upon excitation at 457 nm. In the presence of analyte, TEV protease is produced and cleaves the substrate resulting in fluorescent protein release, loss of FRET-based quenching, and increase in fluorescence intensity of cells. All clones were visually screened for fluorescence increase in the presence of 0.5 mM DNT on LB agar plates (Supplementary Figure SI.2). Colonies that appeared to show increased

fluorescence in the presence of DNT were selected for further screening in liquid medium on 24-well plates. Ratios of fluorescent intensities for cell cultures grown in the presence of DNT to those grown without DNT (the “activation ratio”) were utilized to identify functional switches. Of the 213 colonies screened in aqueous medium, five showed activation ratios (AR) of greater than three and were selected for sequencing. Expression platform sequences and activation ratios observed in cell culture are shown in Supplementary Table SI.1. No homology in the expression platforms was observed, even for switches exhibiting the same activation ratios. Moreover, the length of the expression platforms for these top five switches ranged from 15 to 30 nucleotides. We should note that the number of bases in the randomized sequences corresponding to the expression platforms of the selected clones was often fewer than 30 due to suboptimal purity of the synthetic DNA primers.

Riboswitch Characterization. The clone with the highest activation ratio (clone 2A-2; AR= 9.8) was selected for further characterization. In order to validate the selected riboswitch clone, we performed a time course study of riboswitch activation in cell cultures and cell lysates. To confirm the DNT-dependent increase in TEV protease activity, cell cultures harboring the riboswitch construct were compared to control cells harboring TEV protease-encoding sequence without riboswitch and under the control of a constitutive promoter. The fluorescence intensity, measured at the eGFP emission wavelength, 510 nm, increased over time in control and riboswitch cell cultures in the presence of 0.5 mM DNT and did not show similar changes in the riboswitch cell cultures without analyte (Supplementary Figure SI.3). We noticed that the riboswitch activation ratio of 2.0, calculated in time course studies, was lower than that (9.8) determined in selection experiments. The difference in activation ratios for the same riboswitch construct corresponds with differences in cell growth rates between small and large culture volumes (24-well plate vs culture flask). The growth curves of control and riboswitch cells with and without analyte were similar (Supplementary Figure SI.4), demonstrating that 0.5 mM DNT is nontoxic to the cells and confirming that changes of the spectral profile of these cultures were attributable to riboswitch behavior and do not result from variation in their growth pattern.

We observed a greater riboswitch activation ratio in cell lysates compared to that in cell cultures due to elimination of background fluorescence of the medium. Figure 2 shows the riboswitch activation over time based on the increase in fluorescence intensity at 510 nm. The TEV protease under riboswitch control displayed a 10-fold increase in signal in the presence of DNT over the riboswitch “OFF” state. The riboswitch “ON” curve was similar to positive control (TEV POS CNTRL) when TEV protease was expressed directly. However, we observed increase in the fluorescence intensity of cell lysates without analyte when the riboswitch was in the “OFF” state compared to that for the negative control (FRET NEG CNTRL) in which FRET-based protein was produced and accumulated, but not cleaved by TEV protease. The presence of fluorescence background when the riboswitch was in the “OFF” state indicated the low level of TEV protease expression, even in the absence of analyte, due to riboswitch “leakage” (the inability of the riboswitch to completely maintain the “OFF” state conformation within the cellular system). Surprisingly, the decrease in fluorescence intensity of cells harboring riboswitch without analyte treatment (RS “OFF”)

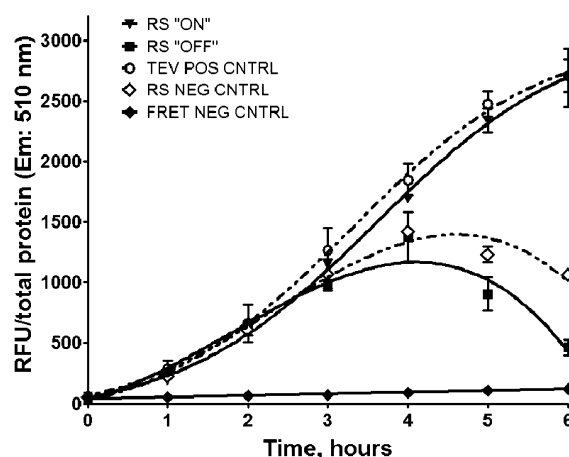


Figure 2. Time course study of riboswitch activation in response to 2,4-dinitrotoluene addition. Emission at 510 nm was monitored in cellular extracts of TOP10 *E. coli* cells harboring FRET-based protein (TEV protease substrate), eGFP-TL-REACH, and one of the following constructs: TEV protease under control of constitutive promoter (TEV POS CNTRL) (white circles); riboswitch-TEV protease in the presence of DNT (RS “ON”) (inverted black triangles); riboswitch-TEV protease (RS “OFF”) (black squares); riboswitch TEV protease in the presence of 4-nitrophenol (RS NEG CNTRL) (white rhombus); and riboswitch-TEV protease inactive mutant (FRET NEG CNTRL) (black rhombus). DNT at 0.5 mM or 0.1 mM 4-nitrophenol was added at time 0, and samples were collected at indicated time points.

occurred at 5 and 6 h time points. The observed decrease in fluorescence intensity of cellular lysates without an analyte did not result from the decrease in the expression of TEV protease substrate. The fluorescence intensity of cells harboring FRET-based protein (TEV protease substrate) and non-active mutant of TEV protease under control of riboswitch was slightly increased over time due to production of FRET-based protein (Supplementary Figure SI.5). We should mention that quenching of eGFP by REACH protein was not 100% in FRET-based construct, and uncleaved fusion protein showed a low fluorescence background. We assume that decrease in production of TEV protease in cells harboring riboswitch construct without an analyte could be a reason for decrease in fluorescence intensity of cellular lysates. Moreover, we observed similar (but not as drastic) decrease in fluorescence intensity of cells harboring riboswitch clone 1B-7 without DNT treatment after the 5 h time point (Supplementary Figure SI.6). Further study of these riboswitches with different reporter proteins will clarify their behavior upon activation in *E. coli* cells. In order to show that the developed riboswitch can be activated only in the presence of DNT, we treated riboswitch-harboring cells with a chemical with properties isomorphic to those of DNT, 4-nitrophenol (riboswitch negative control). 4-Nitrophenol was previously used to test the specificity of TNT aptamer.¹⁵ In experiments with 4-nitrophenol, the concentration of analyte was reduced to 0.1 mM due to toxicity of 0.5 mM 4-nitrophenol to the cells (Supplementary Figure SI.7). The fluorescence profiles of negative control (RS NEG CNTRL) were similar to the profiles of “OFF” state, thus indicating the specificity to DNT in the newly developed riboswitch (Figure 2).

We observed a visual difference between riboswitch “OFF” and “ON” states in cellular lysates of harvested cells. Images of cell lysates at indicated time points (Figure 3A) showed a

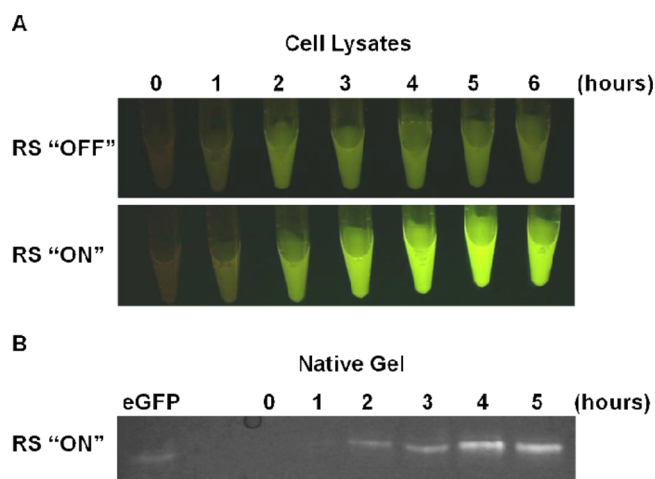


Figure 3. Visualization of DNT dependent riboswitch activation. (A) Images of clarified lysates of cells without DNT treatment (upper panel) and cells exposed to DNT (lower panel) harvested at indicated time points were taken using FUJIFILM digital camera and Dark Reader transilluminator (Clare Chemical Research). (B) A 12% Tris-HCl non-denaturing PAGE shows purified eGFP (0.8 μ g) in the first lane and an aliquot of each lysate (36 μ g of total protein) at indicated time point.

gradual increase in the fluorescence signal of released eGFP due to cleavage of eGFP-TL-REACH by expressed TEV protease in riboswitch-activated cells. The cleavage of the FRET-based protein in cellular lysates of riboswitch-activated cells was demonstrated by appearance of well-defined eGFP corresponding band in non-denaturing polyacrylamide gel (Figure 3B).

In order to investigate thresholds of the detection, we examined the fluorescence signal in response to varying DNT concentrations. For this study we used a range of DNT concentrations, which was based on environmental concentrations in contaminated water (0.04–48.6 mg/L).¹⁷ Presuming that the intracellular concentrations of DNT will be lower than the external concentrations due to limitations in bacterial cell wall permeability,^{31,32} the concentration of DNT corresponded to 0.78 mg/L (4.3×10^{-6} M) was used as the lowest concentration, which is two orders higher than the K_d (1×10^{-8} M) for the analyte binding to the aptamer.¹⁵ As can be observed in Figure 4, the changes in the fluorescence intensity in response to different analyte concentrations demonstrate a typical dose–response curve. We were not able to reach a saturation state at higher concentrations of analyte due to the toxic effects of high concentrations of DNT on cell growth and viability. On the basis of the dose–response curve, the increase in fluorescence intensity can be detected at DNT concentrations as low as 9.1 mg/L, which is in the range of observed environmental concentrations (0.04–48.6 mg/L).¹⁷

Analysis of Switching Mechanism. The secondary structure of the selected riboswitches was analyzed using the Mfold package.²⁷ We calculated the lowest energy structure in “OFF” and “ON” states as well as suboptimal structures. One of the factors that affect an activation ratio is the energy barrier or a difference in free energy between the “OFF” and “ON” states of the riboswitch: if the energy difference between the “OFF” and “ON” states is small, it is very likely that the riboswitch can change into an “ON” state even in the absence of ligand. Qi *et al.* have observed recently an almost linear correlation between the free energy difference and fluorescence intensity in *trans*-acting aptamer-ncRNA regulators in *E. coli* cells.³³ Furthermore,

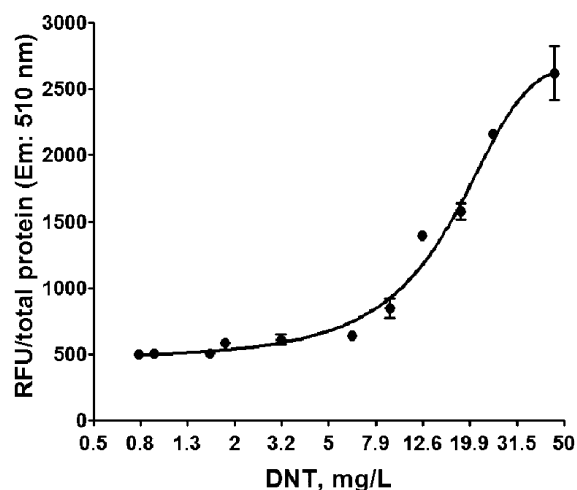


Figure 4. Dose–response graph showing fluorescence of cell lysates 6 h after activation of riboswitch with DNT concentrations ranging from 0.48 to 45.5 mg/L.

as was shown by Beisel and Smolke, free energy difference impacts also the basal level and dynamic range of the riboswitches.³⁴ We have found that riboswitch 2A-2 with the highest activation ratio (AR = 9.8) has an energy barrier of $\Delta G = 5.1$ kcal/mol (Figure 5). The riboswitch 1C-8 has an energy

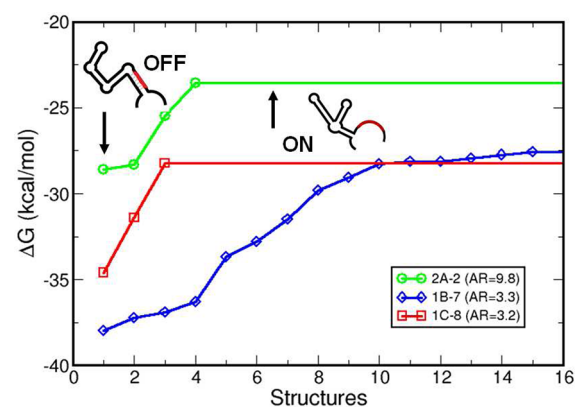


Figure 5. Energy profiles of DNT riboswitches as predicted by Mfold with schematic representation of 2A-A riboswitch in “OFF” and “ON” states. Riboswitch 2A-2 with the highest activation ratio AR = 9.8 has an energy barrier of $\Delta G = 5.1$ kcal/mol, while riboswitch 1C-8 has an energy barrier of 6.2 kcal/mol but activation ratio of only 3.2. Riboswitches 1B-7 and 1C-8 have similar activation ratios or 3.3 and 3.2 but different energy barriers of 11.8 and 6.2 kcal/mol, respectively. However, riboswitch 1C-8 has only one intermediate conformation between the “OFF” and “ON” states, whereas the riboswitch 1B-7 has 14 intermediate conformations. The existence of many intermediate structures makes it easier for the riboswitch to switch from “OFF” to “ON” states.

barrier of 6.2 kcal/mol, but this difference in energy leads to a drop of the activation ratio to 3.2. On the other hand, riboswitches 1C-8 and 1B-7 have very similar activation ratios (3.2 and 3.3) but significantly different energy barrier between the “OFF” and “ON” states, 6.2 and 11.8 kcal/mol, respectively. Therefore, energy barrier alone cannot explain the observed difference in the activation ratio of these riboswitches.

Next, we analyzed the distance or number of intermediate conformations between the “OFF” and “ON” states of the riboswitches. RNA molecules are dynamic systems; they can

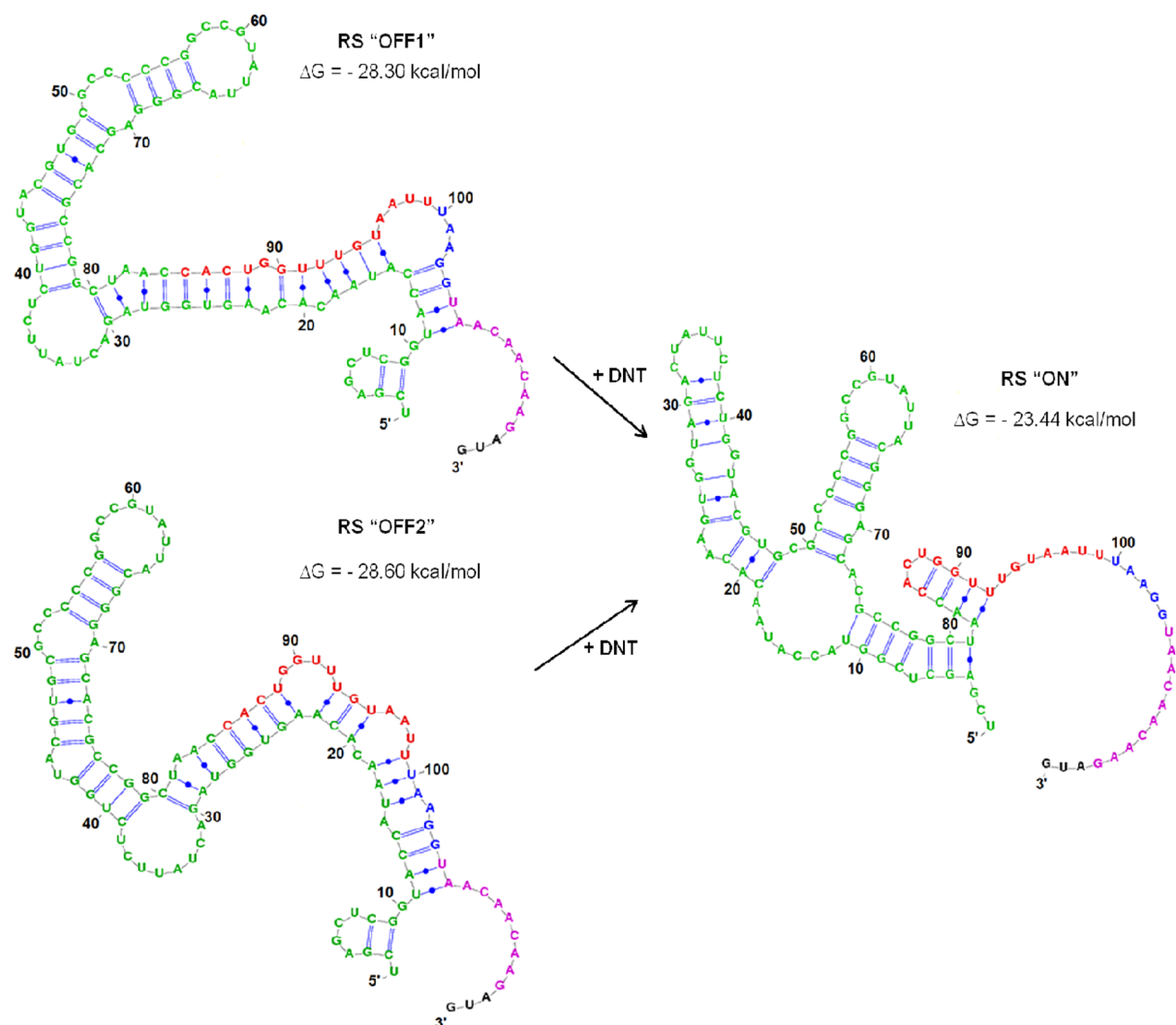


Figure 6. Predicted secondary structure of the DNT 2A-2 riboswitch in the “OFF” and “ON” states. Green = aptamer; red = expression platform; blue = RBS; black = start codon (AUG). There are two conformations of riboswitch in the “OFF” state with difference in energy of 0.3 kcal/mol.

switch from one conformation state to another state that is close in energy. We found that riboswitch 2A-2 has only two intermediate conformations between the “OFF” and “ON” states, whereas the riboswitch 1B-7 has 14 intermediate conformations (Figure 5). We hypothesized that the existence of many intermediate structures makes it easier for the riboswitch to switch from “OFF” to “ON”, thereby lowering the activation ratio. A similar suggestion was made by Hall, Hesselbergth, and Ellington,³⁵ who have shown that both the height of the energy barrier and the distance (number of intermediate states) between the active and inactive conformations affect the level of aptazyme activation.

To clarify the behavior of the developed riboswitch, we investigated the switching mechanism. Relying on examination of the nucleotide sequences of different riboswitch clones (Supplementary Table SI.1), we assumed that the ribosome binding site and the nucleotide sequence neighboring the RBS are involved in hybridization with the aptamer domain in the absence of analyte, resulting in translational repression of downstream gene expression. Analyte binding changes the conformation of the aptamer domain leading to unpairing of the RBS and making the RBS sequence accessible to the ribosome. The translational regulation mechanism for synthetic

riboswitches was previously identified by Gallivan and co-workers^{25,36,37} and Yokobayashi and co-workers.^{26,38}

Mfold software predicted two possible low energy secondary structures for the 2A-2 riboswitch in the “OFF” state with the energies of -28.30 and -28.60 kcal/mol (see Figures 5 and 6). The two conformations share a common secondary structure for bases A23-U88. In the “OFF1” configuration only two bases of RBS are involved in pairing with the aptamer domain, which could cause the fluorescence background in the “OFF” state due to riboswitch “leakage”. Conversely, in the “OFF2” conformation four of the five RBS bases are involved in pairing with aptamer bases, which would lead to lower background fluorescence. In the presence of DNT molecules, the aptamer domain of the riboswitch (colored in green in Figure 6) changes its conformation and binds the ligand. The expression platform becomes less paired, and the RBS is now available for ribosome binding, resulting in translation of TEV protease and increase in fluorescent signal.

Analysis of the secondary structure of the 1B-7 riboswitch shows a similar picture (Supplementary Figure SI.8) but with more intermediate states. In the lowest energy configuration with the energy of folding $\Delta G = -38.0$ kcal/mol, all RBS bases are paired with the aptamer domain and the riboswitch is in the

“OFF” state (Supplementary Figure SI.8A). The second lowest configuration has $\Delta G = -37.23$ kcal/mol and three out of five RBS bases are paired with aptamer bases (Supplementary Figure SI.8B). There are 14 intermediate configurations of the 1B-7 riboswitch between the lowest energy “OFF” structure and configuration in the “ON” state (Supplementary Figure SI.8C).

To investigate the DNT-free (riboswitch in “OFF” state) and DNT-bound (riboswitch in “ON” state) structures predicted by Mfold, we performed *in vitro* enzymatic probing of the 2A-2 riboswitch. *In vitro* transcribed riboswitch mRNA sequence (114 nucleotides) was treated with RNase A, which cleaves single-stranded RNA at the 3'-end of pyrimidine residues, or RNase T1, which cleaves single-stranded RNA at 3'-end of guanosine residues. The RNA fragments were separated and analyzed using a 2100 BioAnalyzer (Agilent). The experimentally observed cleavage sites and the results of enzymatic probing with RNases A and T1 are shown in Supplementary Figures SI.9 and SI.10, respectively. First, we focused on an analysis of the structure of the DNT-free (riboswitch in “OFF” state) conformation. Most of the structural difference between riboswitch in “OFF1” and “OFF2” conformations occurs between nucleotide residues G90 and U100. The presence of a band (Supplementary Figure SI.9D) corresponding to cleavage with RNase A at U98, U99, and U100 (Supplementary Figure SI.9A) is more supportive of riboswitch in “OFF1” conformation, in which the indicated nucleotides are located within an unstructured loop. Another observed band corresponding to cleavage at C19 and U100 (Figure SI.9A) supports the riboswitch “OFF1” conformation. The cleavage with RNase T1 observed at G94 (Supplementary Figures SI.10A and SI.10D) is also more indicative of riboswitch “OFF1” conformation. Although the results of enzymatic probing are more suggestive of riboswitch “OFF1” conformation as a dominating structure, we do not exclude that both conformations could be essential for riboswitch function. Recently, Yokobayashi and co-workers showed that the thiamine pyrophosphate (TPP) sensitive riboswitch in its “OFF” state adopts two distinct structures and that both structures contribute to the observed gene regulation by TPP riboswitch.³⁸ Further mutational analysis of DNT riboswitch and *in vivo* experiments will clarify the importance of two possible riboswitch “OFF” structures for the function of the riboswitch.

Structural analysis of the riboswitch in the presence of DNT (RS “ON”) showed that the most conspicuous difference between cleavage patterns of riboswitch “ON” and riboswitch “OFF” structures occurs near the ribosome binding site (Supplementary Figures SI.9 and SI.10). Appearance of a stronger band around G103-G104 in RNase T1 digestion (Supplementary Figure SI.9D) indicates that the ribosome binding site becomes more susceptible to cleavage in the presence of DNT. The presence of a band corresponding to multiple cleavages with RNase A at C2 and U93, at C13 and U105, at C14 and U105, at U16 and U105, and at U16 and C108 is also suggestive of the accessibility of the RBS in the presence of analyte. The structural predictions and experimental results support the conclusion that availability of the ribosome binding site, as a result of conformational changes, regulates translation of downstream genes in this riboswitch.

Conclusion. We present a design strategy for developing a ligand-inducible translational regulation system in *E. coli* cells. An aptamer selected to bind TNT molecules¹⁵ was linked with

a PCR-generated expression platform library placed upstream of the gene encoding Tobacco Etch Virus protease. Introduction of DNT turns the riboswitch “ON”, producing TEV protease, which cleaves a link between the enhanced green fluorescent protein and a non-fluorescent mutant yellow fluorescent protein resulting in increased fluorescence. The selected riboswitch exhibited a 10-fold increase in fluorescence in the presence of 0.5 mM DNT compared to the system without target. Alternatively, if the objective had been to obtain a riboswitch that turns gene expression off in the presence of DNT, a similar library of riboswitch clones encoding a fluorescent reporter gene downstream of the aptamer and randomized region could have been generated. Selection of the riboswitch would then have been based upon lowest fluorescence in the presence and highest fluorescence in the absence of analyte.

We applied enzymatic probing analysis and secondary structure analysis using Mfold to study the conformational change of the riboswitch in the presence and absence of DNT molecules. The conformational change that occurs in the presence of DNT makes the RBS available for binding, thereby permitting initiation of RNA translation and production of TEV protease. Analysis of the riboswitch in the absence of DNT showed the existence of two distinct conformations in the “OFF” state with very close folding free energy. Similarly, two “OFF” state conformations were recently observed in the synthetic thiamine pyrophosphate riboswitch,³⁸ which indicates both the complex nature and common structural properties of riboswitches.

Riboswitch-enabled cells are a promising environmental sensor for small toxic explosive molecule detection.

METHODS

Materials. Ampicillin, chloramphenicol, dimethyl sulfoxide, rhamnose, 4-nitrophenol (4-NP), and 2,4-dinitrotoluene were purchased from Sigma Chemical Company (St. Louis, MO). PCR primers were obtained from MWG Operon (Huntsville, AL). Phusion DNA polymerase was purchased from New England BioLabs (Ipswich, MA). Difco LB was purchased from Becton, Dickinson and Company (Franklin Lakes, NJ). TOP10 competent *E. coli* were purchased from Invitrogen (Carlsbad, CA). The Tobacco Etch Virus protease gene construct and plasmid pHWG640 were generous gifts from Dr. Helena Berglund from Karolinska Institute, Stockholm, Sweden and Dr. Josef Altenbuchner from the Institute of Industrial Genetics at the University of Stuttgart, Germany, respectively. The plasmid pSAL8.1 was kindly provided by Dr. Justin Gallivan from Emory University, Atlanta, GA. Trinitrotoluene DNA aptamer sequence upstream of TEV protease coding sequence was purchased from DNA 2.0 (Menlo Park, CA).

Plasmid manipulations were performed using chemically competent MAX Efficiency DH5 α *E. coli* cells. Full descriptions of primer sequences and plasmid construction techniques are available in the Supporting Information.

Construction of the Plasmid Library. PCR primers were designed to provide incorporation of up to 30 degenerate bases between the TNT aptamer¹⁵ and the Shine-Dalgarno sequence (ribosome binding site).²⁵ PCR was performed in order to insert the randomized expression platform into the pSAL:TNTaptTEV construct.²⁶ The resulting plasmid library and pHWG640:eGFP-TL-REACH were transformed into *E. coli* TOP10 cells and cells were grown overnight at 37 °C.

Screening of Riboswitch Clones. Each of the riboswitch clones was screened on LB agar plates with and without 0.5 mM DNT. Colonies showing high fluorescence were selected for screening in aqueous medium. Briefly, 24-well plates containing 1 mL/well LB medium, supplemented with ampicillin (100 μ g/mL) and chloram-

phenicol (25 $\mu\text{g}/\text{mL}$), were seeded with 20 μL of overnight culture. Cultures were grown for 2.5 h at 37 $^{\circ}\text{C}$, 220 rpm. Rhamnose was added to each well to a final concentration of 0.4%. Thirty minutes after addition of rhamnose, 2,4-DNT was added to "ON" cultures to a final concentration of 0.5 mM. An equivalent volume of DMSO was added to "OFF" cultures. Absorbance at 600 nm and fluorescence at 510 nm (excitation 457 nm) were measured immediately after addition of DNT, and 6 h later. The activation ratio of each culture was determined by dividing the normalized fluorescence of the "ON" state at 6 h by the normalized fluorescence of the "OFF" state at 6 h.

Time Course Experiments. For time course studies, pHWG640:eGFP-TL-REACH and a TEV protease expressing plasmid, either pSAL:TEV, pSAL:RS2A-2TEV, or pSAL:RS2A-2TEVC151A, were transformed into chemically competent *E. coli* TOP10 cells. Three separate colonies of *E. coli* TOP10 cells harboring either the positive control (pHWG640:eGFP-TL-REACH and pSAL:TEV), riboswitch (pHWG640:eGFP-TL-REACH and pSAL:RS2A-2TEV), or negative control (pHWG640:eGFP-TL-REACH and pSAL:RS2A-2TEVC151A) were picked from LB agar plates containing ampicillin (100 $\mu\text{g}/\text{mL}$) and chloramphenicol (25 $\mu\text{g}/\text{mL}$) and grown overnight at 37 $^{\circ}\text{C}$ in separate flasks containing 50 mL of LB media supplemented with ampicillin (100 $\mu\text{g}/\text{mL}$) and chloramphenicol (25 $\mu\text{g}/\text{mL}$). A 1.5 mL aliquot of the overnight cultures was used to inoculate 150 mL of LB supplemented with ampicillin (100 $\mu\text{g}/\text{mL}$) and chloramphenicol (25 $\mu\text{g}/\text{mL}$). Cultures were grown at 37 $^{\circ}\text{C}$ to an OD_{600} of 0.4–0.5 and induced with 0.4% rhamnose for pHWG640:eGFP-TL-REACH expression. Thirty minutes after induction, cultures harboring positive control, riboswitch, or negative control were treated with 0.5 mM DNT in DMSO, or equivalent volume of DMSO for riboswitch in "OFF" state. OD_{600} of each culture and fluorescence at 510 nm (excitation 457 nm) were measured at time 0 (when DNT or vehicle was added), 1, 2, 3, 4, 5, and 6 h after riboswitch activation. At each time point, 10 mL of culture was collected for cell lysis, protein determination, and fluorescence readings. Cell pellets were stored at -80°C until ready for processing. Cell pellets were resuspended in 0.4 mL of lysis buffer (100 mM Tris-HCl, pH 8.0, 150 mM NaCl, 1 mM MgCl_2) and incubated on ice for 30 min. The buffer was supplemented with lysozyme (0.1 mg/mL), Benzonase Nuclease (10 $\mu\text{L}/10$ mL), and iodoacetamide (8 mM). Cell debris was removed by centrifugation at 14000g for 30 min at 4 $^{\circ}\text{C}$ in an Eppendorf 5417R centrifuge (Fisher Scientific, Pittsburgh, PA). Protein concentrations of the clarified cellular extracts were determined by BCA assay; fluorescence at 510 nm was read, as described above. Riboswitch negative control experiments were performed exactly as above, substituting DNT with 4-nitrophenol at a concentration of 0.1 mM. All time course studies were conducted in triplicate, and data are presented as the mean \pm SEM.

Dose–Response Experiments. Dose–response experiments were performed as described above for time course experiments. DNT was added to the media at various concentrations (0.005, 0.01, 0.05, 0.1, 0.25, and 0.5 mM), and cells were harvested and lysed at time 6 h. Total protein concentrations, fluorescence, and OD_{600} were determined as described above.

Analysis of Secondary Structure of the Riboswitch. The secondary structure of the riboswitch was analyzed using enzymatic probing. Cleavage fragment sizes were predicted manually based on the cleavage specificities of RNases A and T1 (Ambion, Austin, TX). Riboswitch RNA was incubated with or without DNT in Structure Buffer for 15 min at RT prior to addition of RNA-grade ribonucleases. Reactions were carried out according to manufacturer's protocol. Dried sample pellets were resuspended in 10 μL of nuclease-free water and denatured at 70 $^{\circ}\text{C}$ for 2 min prior to analysis on a 2100 BioAnalyzer, using the Small RNA Kit (Agilent, Santa Clara, CA). Peak sizes obtained experimentally were compared to relative likelihood of fragment size occurrence as determined by cleavage analysis of secondary structures predicted by Mfold²⁷ and of the predicted secondary structure provided in Ehrentreich-Förster's publication, which accounts for proximity to TNT.¹⁵

■ ASSOCIATED CONTENT

● Supporting Information

Experimental procedures, growth and fluorescence data, and enzymatic probing analysis. This material is available free of charge via the Internet at <http://pubs.acs.org>.

■ AUTHOR INFORMATION

Corresponding Author

*E-mail: svetlana.harbaugh.ctr@wpafb.af.mil; nancy.kelley-loughnane@wpafb.af.mil.

Present Addresses

[†]UES, Inc., 4401 Dayton-Xenia Road, Dayton, Ohio 45432, United States.

[‡]The Henry M. Jackson Foundation, 6720A Rockledge Drive, Bethesda, Maryland 20817, United States.

Notes

The authors declare no competing financial interest.

This paper has been approved for public release with unlimited distribution.

■ ACKNOWLEDGMENTS

This research was funded by the Air Force Office of Scientific Research (AFOSR).

■ ABBREVIATIONS

DMSO, dimethyl sulfoxide; DNT, 2,4-dinitrotoluene; eGFP, enhanced green fluorescent protein; FRET, fluorescence resonance energy transfer; nt, nucleotide; RBS, ribosome binding site; REACH, resonance energy accepting chromoprotein; RNA, ribonucleic acid; SELEX, Systematic Evolution of Ligands by EXponential Enrichment; TEV, Tobacco Etch Virus; TNT, 2,4,6-trinitrotoluene

■ REFERENCES

- (1) Blouin, S., Mulhbachter, J., Penedo, J. C., and Lafontaine, D. A. (2009) Riboswitches: ancient and promising genetic regulators. *ChemBioChem* 10, 400–416.
- (2) Topp, S., and Gallivan, J. P. (2010) Emerging applications of riboswitches in chemical biology. *ACS Chem. Biol.* 5, 139–148.
- (3) Gu, M. B., and Chang, S. T. (2001) Soil biosensor for the detection of PAH toxicity using an immobilized recombinant bacterium and a biosurfactant. *Biosens. Bioelectron.* 16, 667–674.
- (4) Gu, M. B., Choi, S. H., and Kim, S. W. (2001) Some observations in freeze-drying of recombinant bioluminescent *Escherichia coli* for toxicity monitoring. *J. Biotechnol.* 88, 95–105.
- (5) Mbenkui, F., Richaud, C., Etienne, A. L., Schmid, R. D., and Bachmann, T. T. (2002) Bioavailable nitrate detection in water by an immobilized luminescent cyanobacterial reporter strain. *Appl. Microbiol. Biotechnol.* 60, 306–312.
- (6) Premkumar, J. R., Rosen, R., Belkin, S., and Lev, O. (2002) Sol-gel luminescence biosensors: Encapsulation of recombinant *E. coli* reporters in thick silicate films. *Anal. Chim. Acta* 462, 11–23.
- (7) O'Connor, K., Fletcher, S. A., and Csonka, L. N. (2009) Increased expression of Mg(2+) transport proteins enhances the survival of *Salmonella enterica* at high temperature. *Proc. Natl. Acad. Sci. U.S.A.* 106, 17522–17527.
- (8) Hollands, K., Proshkin, S., Sklyarova, S., Epshtein, V., Mironov, A., Nudler, E., and Groisman, E. A. (2012) Riboswitch control of Rho-dependent transcription termination. *Proc. Natl. Acad. Sci. U.S.A.* 109, 5376–5381.
- (9) Vitreschak, A. G., Rodionov, D. A., Mironov, A. A., and Gelfand, M. S. (2004) Riboswitches: the oldest mechanism for the regulation of gene expression? *Trends Genet.* 20, 44–50.

- (10) Watson, P. Y., and Fedor, M. J. (2011) The glmS riboswitch integrates signals from activating and inhibitory metabolites in vivo. *Nat. Struct. Mol. Biol.* 18, 359–363.
- (11) Tuerk, C., and Gold, L. (1990) Systematic evolution of ligands by exponential enrichment: RNA ligands to bacteriophage T4 DNA polymerase. *Science* 249, 505–510.
- (12) Roth, A., Breaker, R. R. (2004) Selection in vitro of allosteric ribozymes. Ribozymes and siRNA Protocols, in *Methods Mol. Biol.* (Sioud, M., Ed.) 2nd ed., Vol. 252, pp 145–164, Humana Press, Inc., Totowa, NJ.
- (13) Suess, B., and Weigand, J. E. (2008) Engineered riboswitches: overview, problems and trends. *RNA Biol.* 5, 1–6.
- (14) Sinha, J., Topp, S., and Galliva, J. P. (2011) From SELEX to cell dual selections for synthetic riboswitches. *Methods Enzymol.* 497, 207–220.
- (15) Ehrentreich-Förster, E., Orgel, D., Krause-Griep, A., Cech, B., Erdmann, V. A., Bier, F., Scheller, F. W., and Rimmel, M. (2008) Biosensor-based on-site explosives detection using aptamers as recognition elements. *Anal. Bioanal. Chem.* 391, 1793–1800.
- (16) Suski, J. G., Salice, C., Houpt, J. T., Bazar, M. A., and Talent, L. G. (2008) Dose-related effects following oral exposure of 2,4-dinitrotoluene on the Western fence lizard, *Sceloporus occidentalis*. *Environ. Toxicol. Chem.* 27, 352–359.
- (17) Spanggord, R. J., Gibson, B. W., Keck, R. G., and Thomas, D. W. (1982) Effluent analysis of wastewater generated in the manufacture of 2,4,6-trinitrotoluene. 1. Characterization study. *Environ. Sci. Technol.* 16, 229–232.
- (18) Yang, H., Zhao, J.-S., and Hawari, J. (2009) Effect of 2,4-dinitrotoluene on the anaerobic bacterial community in marine sediment. *J. Appl. Microbiol.* 107, 1799–1808.
- (19) Xu, J., and Jing, N. (2012) Effects of 2,4-dinitrotoluene exposure on enzyme activity, energy reserves and condition factors in common carp (*Cyprinus carpio*). *J. Hazard Mater.* 203–204, 299–307.
- (20) Tyson, C. A., Dilley, J. V., Sasmore, D. P., Spanggord, R. J., Newell, G. W., and Dacre, J. C. (1982) Single-dose and repeated-exposure toxicity of a complex wastewater from munitions manufacturing plants. *J. Toxicol. Environ. Health* 9, 545–564.
- (21) Lent, E. M., Crouse, L. C., Quinn, M. J., Jr., and Wallace, S. M. (2012) Comparison of the repeated dose toxicity of isomers of dinitrotoluene. *Int. J. Toxicol.* 31, 143–157.
- (22) Klaassen, C. D., Ed. (2001) *Casarett & Doull's Toxicology: The Basic Science of Poisons*, 6th ed., 1236 p, New York: McGraw-Hill.
- (23) Ganesan, S., Ameer-beg, S. M., Ng, T. T., Vojnovic, B., and Wouters, F. S. (2006) A dark yellow fluorescent protein (YFP)-based Resonance Energy-Accepting Chromoprotein (REACH) for Förster resonance energy transfer with GFP. *Proc. Nat. Acad. Sci. U.S.A.* 103, 4089–4094.
- (24) Harbaugh, S., Kelley-Loughnane, N., Davidson, M., Narayanan, L., Trott, S., Chushak, Y. G., and Stone, M. O. (2009) FRET-based optical assay for monitoring riboswitch activation. *Biomacromolecules* 10, 1055–1060.
- (25) Lynch, S. A., and Gallivan, J. P. (2009) A flow cytometry-based screen for synthetic riboswitches. *Nucleic Acids Res.* 37, 184–192.
- (26) Nomura, Y., and Yokobayashi, Y. (2007) Reengineering a natural riboswitch by dual genetic selection. *J. Am. Chem. Soc.* 129, 13814–13815.
- (27) Zuker, M. (2003) Mfold web server for nucleic acid folding and hybridization prediction. *Nucleic Acids Res.* 31, 3406–3415.
- (28) Rickert, D. E., Butterworth, B. E., and Popp, J. A. (1984) Dinitrotoluene: acute toxicity, oncogenicity, genotoxicity, and metabolism. *Crit. Rev. Toxicol.* 13, 217–233.
- (29) Banerjee, H. N., Verma, M., Hou, L.-H., Ashraf, M., and Dutta, S. K. (1999) Cytotoxicity of TNT and its metabolites. *Yale J. Biol. Med.* 72, 1–4.
- (30) Hanahan, D. (1983) Studies on transformation of *Escherichia coli* with plasmids. *J. Mol. Biol.* 166, 557–580.
- (31) Nikaido, H. (1993) Transport across the bacterial outer membrane. *J. Bioenerg. Biomembr.* 25, 581–589.
- (32) Nikaido, H. (2003) Molecular basis of bacterial outer membrane permeability revisited. *Microbiol. Mol. Rev.* 67, 593–656.
- (33) Qi, L., Lucks, J. B., Liu, C. C., Mutalik, V. K., and Arkin, A. P. (2012) Engineering naturally occurring *trans*-acting non-coding RNAs to sense molecular signals. *Nucleic Acids Res.* 20, 5775–5786.
- (34) Beisel, C. L., and Smolke, C. D. (2009) Design principles for riboswitch function. *PLoS Comput. Biol.* 5, 1–14.
- (35) Hall, B., Hesselberth, J. R., and Ellington, A. D. (2007) Computational selection of nucleic acid biosensors via a slip structure model. *Biosens. Bioelectron.* 22, 1939–1947.
- (36) Lynch, S. A., Desai, S. K., Sajja, H. K., and Gallivan, J. P. (2007) A high-throughput screen for synthetic riboswitches reveals mechanistic insights into their function. *Chem. Biol.* 14, 173–84.
- (37) Sinha, J., Reyes, S. J., and Gallivan, J. P. (2010) Reprogramming bacteria to seek and destroy an herbicide. *Nat. Chem. Biol.* 6, 464–470.
- (38) Muranaka, N., Sharma, V., and Yokobayashi, Y. (2011) Enzymatic probing analysis of an engineered riboswitch reveals multiple off conformations. *Nucleosides, Nucleotides Nucleic Acids* 30, 696–705.